Chemical Geology 269 (2010) 113–123

Contents lists available at ScienceDirect

Chemical Geology

journal homepage: www.elsevier.com/locate/chemgeo

Kinetics of selenium release in mine waste from the Meade Peak Phosphatic Shale, Phosphoria Formation, Wooley Valley, Idaho, USA

Lisa L. Stillings [a,*], Michael C. Amacher [b]

[a] U.S. Geological Survey, MS-176, University of Nevada, Reno, Reno, NV 89557, United States
[b] U.S. Forest Service, Rocky Mountain Research Station, Forestry Sciences Lab, 860 N 1200 E, Logan, UT 84321, United States

ARTICLE INFO

Article history:
Received 23 February 2009
Received in revised form 23 October 2009
Accepted 26 October 2009

Keywords:
Selenium
Oxidation kinetics
Leaching
Black shale
Marine shale
Phosphoria Formation

ABSTRACT

Phosphorite from the Meade Peak Phosphatic Shale member of the Permian Phosphoria Formation has been mined in southeastern Idaho since 1906. Dumps of waste rock from mining operations contain high concentrations of Se which readily leach into nearby streams and wetlands. While the most common mineralogical residence of Se in the phosphatic shale is elemental Se, Se(0), Se is also an integral component of sulfide phases (pyrite, sphalerite and vaesite–$pyrite_{ss}$) in the waste rock. It may also be present as adsorbed selenate and/or selenite, and $FeSe_2$ and organo-selenides.

Se release from the waste rock has been observed in field and laboratory experiments. Release rates calculated from waste rock dump and column leachate solutions describe the net, overall Se release from all of the possible sources of Se listed above. In field studies, Se concentration in seepage water (pH 7.4–7.8) from the Wooley Valley Unit 4 dump ranges from 3600 µg/L in May to 10 µg/L by Sept. Surface water flow, *Q*, from the seep also declines over the summer, from 2 L/s in May to 0.03 L/s in Sept. Se flux ([Se]*Q) reaches a steady-state of <150 mg/day in 1–4 months, depending upon the volume of *Q*. Se release (mg/L) follows a first order reaction with a rate constant, $\boldsymbol{k}$, = 1.35 – 6.35e−3 h^{-1} (11.8–55.6 yr^{-1}).

Laboratory experiments were performed with the waste shale in packed bed reactors; residence time varied from 0.09 to 400 h and outlet pH ~ 7.5. Here, Se concentration increased with increasing residence time and release was modeled with a first order reaction with $\boldsymbol{k}$ = 2.19e−3 h^{-1} (19.2 yr^{-1}).

Rate constants reported here fall within an order of magnitude of reported rate constants for oxidation of Se (0) formed by bacterial precipitation. This similarity among rate constants from both field and laboratory studies combined with the direct observation of Se(0) in waste shales of the Phosphoria Formation suggests that oxidation of Se(0) may control steady-state Se concentration in water draining the Wooley Valley waste dump.

Published by Elsevier B.V.

1. Introduction

An elevated concentration of selenium, Se, in the environment is a critical concern due to its link with deaths, deformities, and birth defects in waterfowl, wildlife, and domestic stock. Much of the attention has been focused on drainage water from agricultural lands, because Se-rich irrigation drainage in the Kesterson Reservoir, CA, caused significant waterfowl mortality and deformity in the early-mid 1980s (Presser, 1994). Indeed, many agricultural lands in the western U.S. are underlain by Se-rich, Cretaceous marine shales and exhibit elevated Se concentrations in associated surface water, bottom sediments, and biota samples (Engberg and Sylvester, 1993; Seiler et al., 2003). Weathering of exposed Cretaceous shales has been cited as the major source of Se to the environment (McNeal and Balistrieri, 1989).

Irrigation of agricultural land is not the only pathway for mobilization and transport of Se, however. Other activities that release Se to the environment include coal mining and combustion; gold, silver, and phosphate mining; metal smelting; municipal landfills; and oil transport, refining, and utilization (Lemly, 2002). This present paper focuses on the magnitude and rate of release of Se from phosphate mining activities in the Permian-aged Phosphoria Formation.

The Phosphoria Formation is a marine black shale that occurs in a 350,000 km^2 region in Idaho, Wyoming, Montana, Utah, and Nevada, and forms one of the largest occurrences of phosphate rock in the world (Hein et al., 2004). Phosphate mining began in the region in 1906 and continues to the present day. However, in addition to the abundant phosphate component in the shale (up to 20% in the Meade Peak Member of the unit), the Phosphoria also contains trace elements associated with the marine components. These elements, including Ag, Cd, Cr, Cu, Mo, Ni, Se, V, and Zn, were associated with the marine plankton that comprised much of the organic fraction of the sediment when it was originally deposited in a shallow marginal sea (Piper, 1999; Hein et al., 2004). Elevated concentrations of these trace elements, and

* Corresponding author. Tel.: +1 775 784 5803.
E-mail address: stilling@usgs.gov (L.L. Stillings).

0009-2541/$ – see front matter. Published by Elsevier B.V.
doi:10.1016/j.chemgeo.2009.10.011

phosphate, were produced due to the loss of ~90% of the host organic matter during diagenesis, from retention of nutrients (phosphate) by the sediment, and because of low influx of other, diluting, terrigenous sediments (Piper, 2001).

Phosphorite rock within the Phosphoria Fm. contains an average Se concentration of 30 mg/kg, with a maximum concentration of 800 mg/kg. Associated mudstones have an average concentration of 14 mg/kg and a maximum concentration of 1500 mg/kg Se (Buck and Jones, 2002). Mining activities over the past century have amplified the natural release of potentially toxic trace elements, including Se, to the environment.

Release of Se has been a major concern in southeast Idaho. In 1996, several horses pastured near a phosphate waste dump were euthanized due to severe selenium toxicosis. Since then many more horses and a few hundred sheep have died from eating Se contaminated forage. Aquatic invertebrates, salamanders, and birds have been found with high concentrations of Se, and advisories for human consumption of fish and elk livers have been issued (Tetra Tech EM Inc., 2002; Greater Yellowstone Coalition, 2006).

Several management strategies to limit Se release have been suggested and adopted by mining companies and land managers in southeastern Idaho. These include new designs of waste dumps to limit water flow to seleniferous materials, changes in seed mixtures for revegetating slopes, and soil amendments for limiting Se uptake by plants (Agrium et al., 2005; Mackowiak and Amacher, 2008). In order to design treatment methods for Se in drainage from the waste dump it is first necessary to estimate the magnitude of Se release over time. Our experiments were designed to measure the rate constant of Se release from the waste rock produced as a byproduct of phosphate mining in southeastern Idaho.

2. Methods

2.1. Laboratory experiments

2.1.1. Materials

The black shale used in these experiments was a bulk composite sample collected from an exposed outcrop of the Meade Peak Member of the Phosphoria Formation at Maybe Canyon in southeastern ID. Previous chemical analyses of this sample determined a total Se concentration of 111 mg/kg, oxalate extractable Se of 27.8 mg/kg, and saturated paste water extractable Se of 0.72 mg/kg (Mackowiak and Amacher, 2008).

Shale samples were prepared by sieving to <0.25 in. (0.635 cm) in the field and air-drying at ambient temperature in trays on greenhouse benches. The sample was not sieved to a range of grain sizes; this was unnecessary because the sample disaggregated upon wetting.

2.1.2. Experimental set-up

Plug flow reactors (also called packed bed reactors; flow cells from Soil Measurement Systems, Tucson, AZ) were used for the experiments (Fig. 1). Several reactor sizes (Table 1) were employed in order to provide a range of residence times, necessary for data analysis. The inflow solution (Fig. 1) was deionized water, equilibrated with atmosphere (pH ~5.7). Flow rates, ranging from 1.8 to 36 $cm^3\ h^{-1}$ (Table 1), were controlled by a Soil Measurement Systems syringe pump. No evidence of back pressure was observed. Reaction progress was monitored with real-time specific conductivity measurements of the outlet solutions, using a Thermo Orion model 135A conductivity meter with temperature-compensated electrode calibrated with 0.01 M KCl (1413 µS at 25 °C). Solutions were then filtered (<1 µm with glass-fiber syringe filters) acidified, and refrigerated for later analysis of Se concentration with hydride generation atomic adsorption spectrometry (HGAAS). The detection limit for the HGAAS is approximately 0.5 µg/L Se. Quality control samples included internal standards, reagent and method blanks, and sample duplicates.

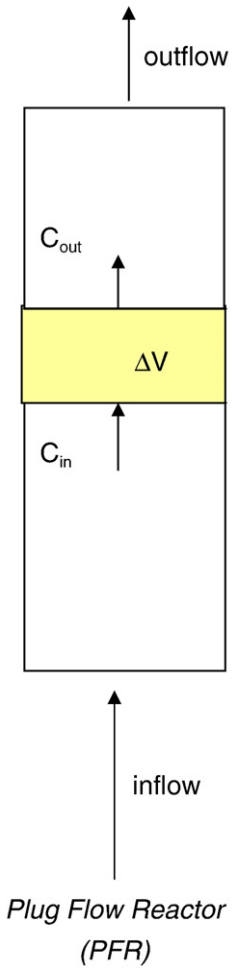

Fig. 1. Schematic of the plug flow reactors used in this study. The mass balance (Eq. (1)) is written for a differentially thin package of fluid, ΔV, and then integrated along the length of the column. C_{in} and C_{out} are concentrations in fluid flowing into and out of the volume element, ΔV, respectively.

2.1.3. Data analysis

A plug flow reactor (PFR) can be visualized with a schematic (Fig. 1) whereby the reaction between a fluid and the solid occurs within a differentially thin package of fluid (volume = ΔV) that moves as a unit, longitudinally through the reactor (Hill, 1977). The movement of the element of interest, Se, through the system is described with a mass balance equation:

Influx	−	Outflux	+	Rate of change by reaction	=	Rate of accumulation	
F_{in}	−	F_{out}	+	R	=	ΔC	(1)

Flux is the product of volumetric flow rate times concentration (***Q*C***), and ***R*** is positive for products and negative for reactants. If we assume a first order reaction, then ***R = k*C***, where ***k*** is the rate constant (h^{-1}). Therefore, the mass balance on the thin package of fluid (***ΔV***; Fig. 1) can be written as:

$$QC|_V - QC|_{V+\Delta V} + \Delta V k(C^* - C) = \Delta V \frac{\partial C(v,t)}{dt} \quad (2)$$

QC|V flux of Se into the volume element, mg h^{-1}
QC|V + ΔV flux of Se out of the volume element, mg h^{-1}
ΔVk(C* − C) the rate of addition of Se to the fluid, due to reaction, mg h^{-1}, where

Table 1
Physical characteristics of the plug flow reactors. Numbers in columns f, g, and h were calculated by the indicated formulas.

Column	a Inside diameter (cm)	b Length (cm)	c Volume (cm^3)	d Flow rate ($cm^3\ h^{-1}$)	e Shale mass (g)	f Bulk density ($g\ cm^{-3}$) (e ÷ c)	g Pore volume (cm^3) ((1−f ÷ 2.65) × c)[a]	h Residence time, τ (h) (g ÷ d)
Micro	0.9	10.50	6.68	36.0	9.33	1.40	3.16	0.0878
Small, 0–37 days	2.54	15.24	77.2	2.53	90.69	1.18	43.0	17.0
Small, 38–41 days	2.54	15.24	77.2	1.79	90.69	1.18	43.0	24.0
Small, 42–100 days	2.54	15.24	77.2	2.15	90.69	1.18	43.0	20.0
1	2.54	7.62	38.6	1.86	52.91	1.37	18.6	10.0
2	2.54	15.24	77.2	1.84	107.22	1.39	36.7	20.0
3	2.54	30.48	154	1.87	192.44	1.25	81.8	43.7
4	7.62	7.62	347	1.89	439.71	1.27	181	96.0
5	7.62	15.24	695	1.85	937.39	1.35	341	184
6	7.62	30.48	1390	1.86	1705.36	1.23	746	401

[a] porosity is calculated as $\phi = 1 - \rho_b/\rho_s$, where ρ_b = bulk density and ρ_s = particle density (assumed to be 2.65 g/cc; Flint and Flint, 2002). Pore volume in the column is then calculated as ϕ*column volume.

ΔV is the volume of fluid in the thin package (Fig. 1), cm^3,
C* is the total concentration of reactive Se in the system, mg cm^{-3}
C is the concentration of Se in the bulk solution, mg cm^{-3}, hence
(C*−C) is the concentration of reactive Se at the solid:solution interface, mg cm^{-3}

At steady-state, the concentration gradient of Se within the reactor does not change, hence $\frac{\partial C(v,t)}{dt} = 0$. By making this substitution and dividing by ***ΔV***, Eq. (2) becomes

$$Q\frac{dC(v)}{dV} = -k(C^*-C) \tag{3}$$

Integrating over the volume of the entire column (and noting that the concentration of Se in the inlet solution = 0 mg cm^{-3}):

$$\int_{Cin}^{Cout}\frac{dC(v)}{C^*-C} = -k\int_0^V \frac{1}{Q}dV \tag{4}$$

$$\ln\frac{C^*-C_{out}}{C^*-0} = -k\frac{V}{Q} = -k\tau \tag{5}$$

Where τ = residence time, $\frac{V}{Q}$, h.

There are 2 unknowns in Eq. (5): ***C**** and ***k***. Performing experiments at different flow rates will produce a dataset where C_{out} is measured as a function of τ. A minimum of two experiments are needed to solve Eq. (5) for ***C**** and ***k***.

2.2. Field measurements

2.2.1. Site

"Field" rates of Se leaching were measured at a wetland in the Caribou National Forest, southeast Idaho (Fig. 2). The wetland formed from seepage at the base of a mine waste rock pile named Wooley Valley Unit 4 (WVU4). The Wooley Valley mine is currently inactive, but had been mined by Rhodia, Inc. (Herring et al., 2001). The material in the dump consisted of the "lower", "middle," and "upper" waste shales that are located stratigraphically below, between, and above, the two phosphate ore zones of the Meade Peak, respectively. Other rock included in the waste dumps may be the Rex Chert, which conformably overlies the Mead Peak member, and the Grandeur Tongue dolomite of the Park City Formation. Se concentrations in the samples from the waste shales range from 7 to 727 mg/kg (Herring et al., 2001), while concentrations in the Rex Chert and Grandeur Tongue are 0.1–138 mg/kg (mean = 12; Hein et al., 2002), and 0.6–47 mg/kg (Herring et al., 2001), respectively. Soils developed on the lifts and terraces of the dumps contain 30–140 mg/kg Se (Amacher et al., 2001).

Because of the snow pack and springtime mud, the field site was rarely accessible before early May. In 2002, field data were collected from May 5 until June 14, at which time the seep dried up and surface flow ceased. In 2006, data were collected from May 12 through October 4; in 2008, from May 20 through October 2.

2.2.2. Data collection

2.2.2.1. Flow measurements. In order to measure Se flux from the waste pile, time series data were collected for both chemical analysis and water discharge from the seep (Fig. 2, point e). In 2002, discharge was measured by two methods: first, discrete measurements of flow were made using a Marsh-McBirney™ meter to record stream velocity, then multiplying by the cross-sectional area of the stream draining from the area of seepage (Carter and Davidian, 1968). Second, an Aquarod™ datalogger was used to measure stream stage as a function of time. Water level was converted to flow through the use of a rating curve of flow vs. stage, established at other locations in the wetland:

$$Q = 3.8\times10^{-13}\cdot(WL)^{3.248} \tag{6}$$

Where Q = water flow, $m^3\ s^{-1}$, and WL = water level, mm.

In 2006 and 2008, the velocity meter/cross-sectional area method was also used to make discrete measurements of water flow. The Aquarod™ was used to record water level as a function of time, but instead of using the rating curve (Eq. (6)) to calculate flow, a 1 in. Parshall flume was installed on the stream, and the following equation, provided by the manufacturer, was used to calculate flow:

$$Q = 0.0283\cdot[0.676\cdot(0.00328\cdot WL)^{1.55}] \tag{7}$$

Where Q = water flow, $m^3\ s^{-1}$, and WL = water level, mm, measured by the Aquarod™.

2.2.2.2. Sample collection and analysis. Surface water samples were automatically collected daily with Sigma™ (2002) or every other day with Isco™ (2006, 2008) automatic samplers. These were visited on a ~3 week frequency, at which time full sample bottles were removed and new ones deployed. Samples were then transported to the laboratory for filtration (0.45 µm mixed cellulose ester (MCE) membrane) and acidification (1%HNO_3). Samples were analyzed by ICP-MS (in 2002; Lamothe et al., 2002) and ICP-AES (in 2006, 2008; Briggs, 2002). Detections limits for these methods are 0.2 and 15 µg/L Se, respectively.

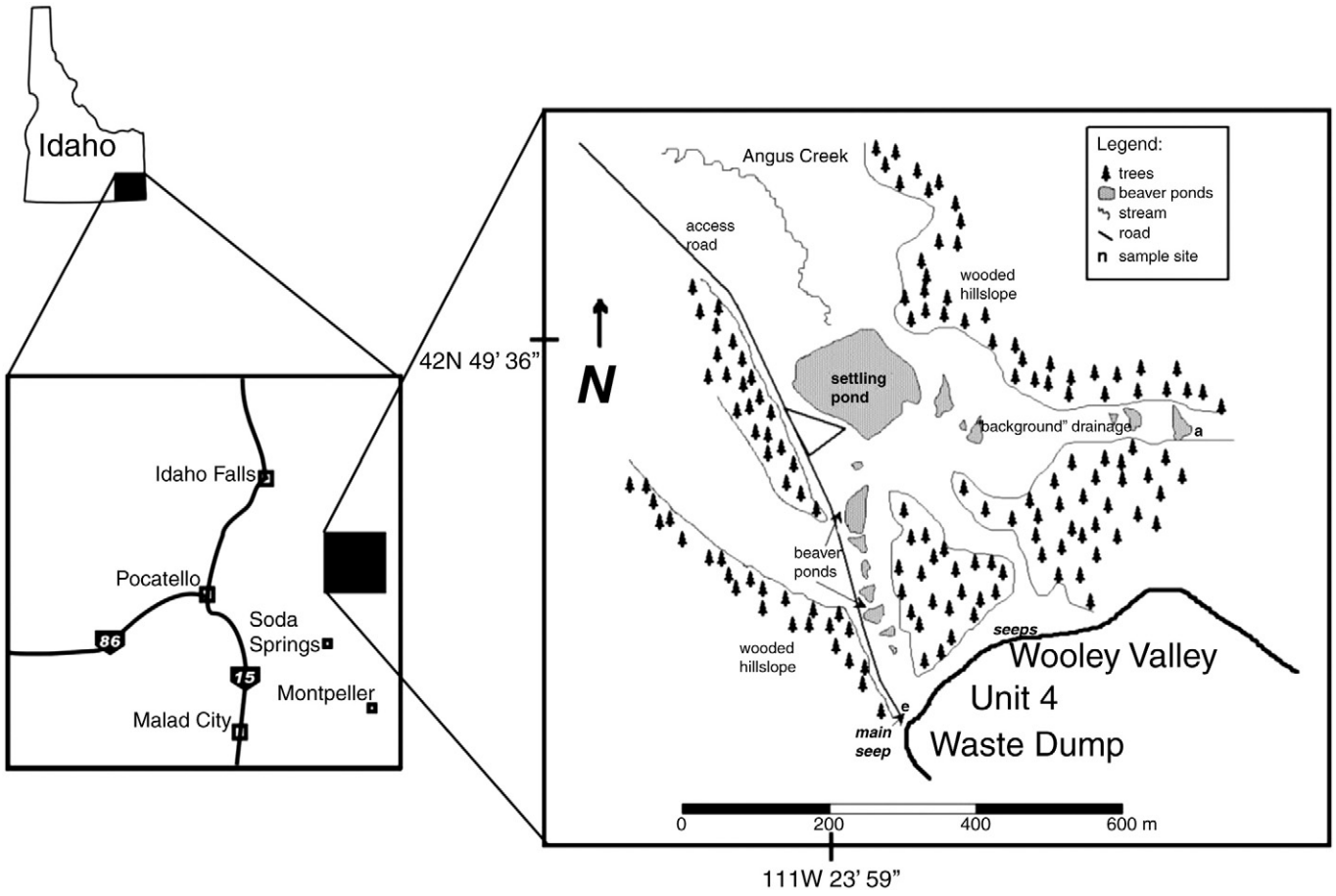

Fig. 2. Location map and schematic for the Wooley Valley Unit 4 waste dump and wetland, after Stillings and Amacher, 2004. Stream flow and Se concentrations were measured immediately downstream of the main seep, point e. Stream water flowed northward from the main seep to the settling pond, then into Angus Creek.

Because water samples remained in the plastic autosampler bottles for 3 weeks before collection, filtration, and acidification, there is a possibility of sample degradation and/or Se adsorption to container walls. This possibility was evaluated by comparing Se concentration in samples collected immediately before and after the date of sample bottle retrieval and redeployment. The last sample in the tray of full bottles was collected the morning of the site visit, and filtered/acidified upon return to the lab; hence there was a short time between sample collection and processing. The first sample collected in the bottle tray after a site visit and bottle redeployment experienced the longest time between collection and processing; hence it had the greatest possibility for sample degradation and Se loss. The variation in Se concentrations between these samples ranged from ~5–40% and did not appear to be much greater than concentration variation observed among samples within a sample tray. We conclude that while sample degradation is always a possibility when automatic samplers are used, Se concentrations in samples collected before and after site visits are within sample method/analytical error.

Seep chemistry and discharge measurements are to be published as a U.S. Geological Survey Open-File Report (Stillings and Amacher, submitted for publication).

3. Results

3.1. Laboratory experiments

In all experiments and reactors, selenium concentration was high in the initial outlet samples and decreased, over time, to a constant value (Fig. 3). In the micro column experiment, the fluid pump was stopped at 168 h, when Se reached a steady-state concentration of 5.2 ± 0.83 µg/L. The shale remained wet, in the column, until 2856 h when the fluid flow was resumed. Upon resumption, Se concentration quickly reached a peak of 124 µg/L, before it slowly decreased to another steady-state concentration of 1.7 ± 1.3 µg/L.

A strong relation was noticed between specific conductivity values of the outlet solutions and Se concentration in the micro and small column experiments (Figs. 3, 4). Therefore, for the column 1–6 experiments, specific conductivity was used to estimate Se concentration, with the following expression:

$$\log[Se] = (SC^{0.48} - 60^{0.48})^{0.35} \quad (8)$$

Where log[Se] = the logarithm of Se concentration (µg/L), and SC = specific conductivity (µS/cm). In fitting the specific conductivity data (Fig. 4), a model was chosen that most accurately fit the data for low specific conductivity, because it is the low conductivity data which define steady-state concentrations (Table 2).

3.2. Field experiments

In the early 2000s, southeastern ID experienced several dry years with little snowfall. Hence, data for flow and Se concentration at the Wooley Valley seep were only available for 2002, 2006 and 2008 (Fig. 5a, b). In 2002 data collection began on May 8 and continued through June 12, when the flow at the seep ceased. Subsequent winters with low snow pack caused minimal flows at the seep. However the winters of 2006 and 2008 were wet enough for the seep to begin flowing again,

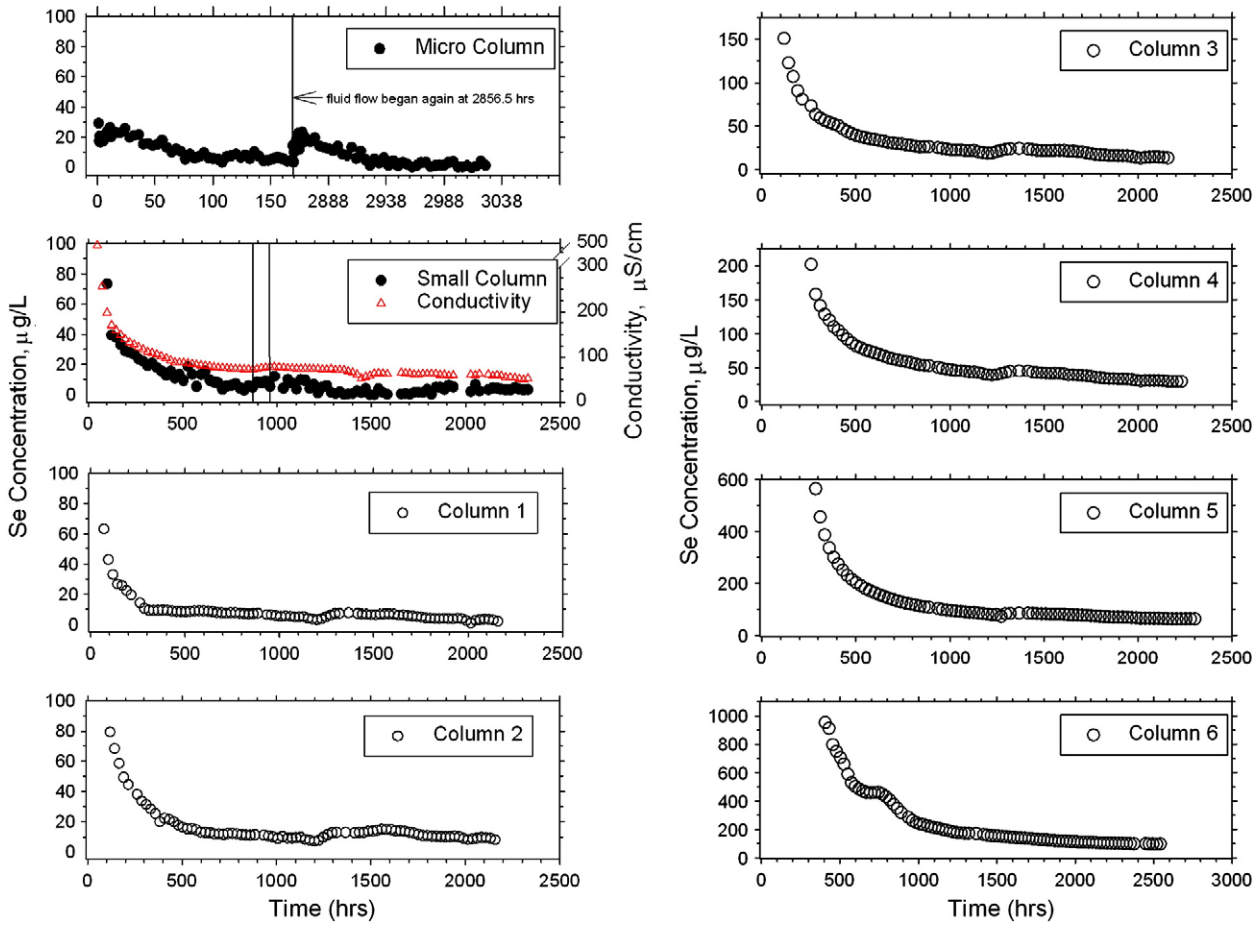

Fig. 3. Concentration of Se versus time, for all experiments. Closed symbols represent Se concentrations determined from HGAAS. Open symbols denote Se concentrations calculated from specific conductivity measurements. Vertical lines on the micro and small column plots indicate a change in flow rate or an interruption of the experiment.

hence data collection continued from May through October, in 2006 and 2008.

In all years, Se concentration dropped exponentially over time (Fig. 5b). In 2002, Se concentration, [Se], in outflow from the seep dropped from 3600 µg/L on May 9 to ~50 µg/L on June 9. The range in concentration was not as great in 2006 and it decreased more slowly over time. The high was ~1200 µg/L on May 14; this dropped to ~10 µg/L on Oct. 3. In 2008 [Se] was 2700 µg/L on May 20, and this dropped to 16.5 µg/L by Oct. 2. Despite differences in the initial Se concentration and flow discharge among 2002, 2006, and 2008, the total mass of Se leached from the waste rock during these periods did not vary greatly, being 570, 810, and 640 g, respectively (Fig. 5c). In 2002, the initial daily flux was measured at 60 g Se/day, in 2006 and 2008 it was 70 and 100 g Se/day, respectively.

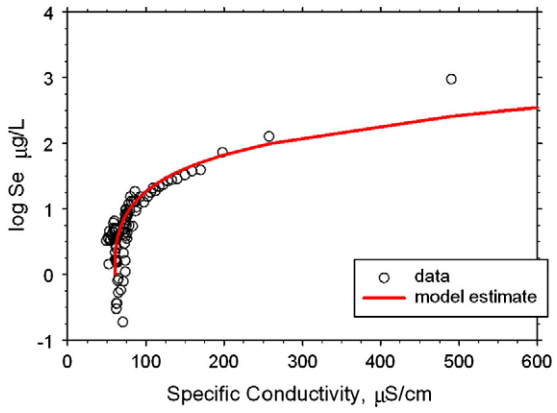

Fig. 4. Relationship between log Se concentration and specific conductivity. Data points were measured from the small column experiment.

4. Discussion

4.1. Laboratory experiments

Data from the column leaching experiments were analyzed with the procedure described in the Methods section, above. First a "steady-state" concentration was determined from each experiment, where "steady-state" was defined as a constant concentration over time. In practice, Se concentrations in the outlet solutions were never completely invariant, so the steady state concentration is expressed as a mean and standard deviation for several data points at the end of each experiment (Table 2).

In a plug flow reactor, the steady-state outlet concentration will be a function of the reaction rate and the residence time of the fluid in the reactor. A plot of steady-state concentration vs residence time (Fig. 6a) shows that outlet, steady-state concentration increases with increasing residence time. A linear model fits the data with an r^2 of 0.979. By selecting τ and C ($[Se]_{s-s}$) from any two points on the line, Eq. (5) can be solved for the rate constant $\boldsymbol{k}$ (2.19e−3 h^{-1}), and the amount of reactive Se in the system, $\boldsymbol{C^*}$ (170 µg/L). While Fig. 6a describes the physical relationship between residence time and steady-state concentration, the kinetic expression of Eq. (5) can be illustrated in Fig. 6b, where the negative slope of the line is the rate constant.

It must be noted that this rate constant describes an overall, steady-state reaction. Examination of $[Se]_{outlet}$ as a function of time (Fig. 3)

Table 2
Steady-state time period, Se concentration ($[Se]_{s-s}$), and specific conductivity (SC_{s-s}) in the outflow of each reactor. The value 'n' is the number of samples used to calculate mean $[Se]_{s-s}$; the time period is the interval over which steady-state was observed.

Column	$Time_{s-s}$ h	pH_{outlet}	$[Se]_{s-s}$ μg/L mean	$[Se]_{s-s}$ μg/L stand dev	SC_{s-s} μS/cm mean	SC_{s-s} μS/cm stand dev	*n*
Micro	144–168	7.5	5.2	0.8			7
Micro	2940–3024	7.5	1.7	1.3			17
Small, 0–37 days	712–872	7.6	5.1	1.4	73.6	1.2	8
Small, 38–41 days	895–864	7.4	7.7	1.4	75.8	2.2	4
Small, 42–100 days	2120–2304	7.4	3.8	0.5	55.2	3.9	9
1	1990–2159	7.5	2.7*	0.8	53.9	1.1	8
2	1990–2159	7.4	8.9*	0.5	76.0	1.3	8
3	1990–2159	7.5	13.7*	0.4	88.4	1.2	8
4	1990–2231	7.7	30.4*	0.8	132	1.9	11
5	2183–2303	7.8	63.3*	0.2	212	0.5	6
6	2351–2543	7.9	98.3*	0.9	290	2.0	7

*$[Se_{s-s}]$ calculated from SC_{s-s}, Eq. (8).

shows that in every experiment $[Se]_{outlet}$ is initially high, and then drops to a much lower, steady-state concentration. Moreover, when flow is resumed after a period of drying, $[Se]_{outlet}$ will peak before beginning another exponential decline.

This observation, of an initially high [Se] followed by a low, steady-state [Se] suggests that it is the highly soluble form of Se that is first released from the shale, followed by a slower release of Se from a less soluble, refractory source. Selenium can be found in a variety of forms within the shale waste rock: it may be found in various redox species, Se(−II), Se(0), Se(IV), and Se(VI), it may be adsorbed to mineral surfaces, found in salts, associated with organics, substituted for S in sulfides, and perhaps found as elemental Se(0), a product of bacterial oxidation (Dowdle and Oremland, 1998; Losi and Frankenberger, 1998). Ryser et al., 2005, 2006, observed multiple oxidation states for Se (Se(−II,0), Se(IV), and Se(VI)) in waste rock from the phosphate mines in southeast Idaho. Perkins and Foster, 2004, observed Se to be associated with oxyhydroxides in weathered sections of the Phosphoria Fm., and associated with sulfides and as elemental Se in unweathered sections.

Highly soluble Se might be found in easily hydrolyzed salts, and/or as species adsorbed to mineral surfaces. Numerous studies have shown that adsorption/desporption reactions have fairly rapid kinetics, and that rate constants for these reactions are on the same order as those for the release of water from hydration shell of metals in solution (Hachiya et al., 1984, Zhang and Sparks, 1989; van Leeuwen, 2008). While these reactions may contribute Se to the initial outlet solution of the laboratory soil columns, the adsorption reactions should be at equilibrium once steady-state is obtained (i.e. constant pH and Se concentration). Studies of Se speciation in the Kesterson soils show that the most soluble Se species are Se(VI) and Se(IV), with Se(VI) having the greatest solubility because it does not adsorb to mineral surfaces as strongly as Se(IV). Several studies demonstrate that it is the oxidized, highly soluble Se which is rapidly released from soils, and that longer-term release is governed by oxidation of more refractory species, such as Se(0), and Se associated with sulfides (Masscheleyn et al., 1990; Tokunaga, et al., 1994, 1996; Zawilslanski and Zavarin, 1996; Martens and Suarez, 1997; Losi and Frankenberger, 1998; Zawislanski et al., 2003). In the experiments presented here, Se concentrations from the long term, steady-state release were used to calculate the rate constant. It is reasonable to assume that this rate constant reflects oxidation of a refractory Se species, such as Se(0) or Se-bearing sulfides.

Grauch et al., 2004, examined shales of the Meade Peak member with a combination of optical microscopy, SEM, and electron microprobe techniques. They concluded that although Se is found associated with sulfides (pyrite, sphalerite, and vaesite–$pyrite_{ss}$), the predominate Se-bearing solid phase is native Se, Se(0), found in grains of <2 μm. Textural relationships suggest that the grains of Se(0) grew by filling in pore spaces after catagenesis. Ryser et al., 2005, identified dzharkenite, FeSe2, a di-selenide carbon compound, Se-substituted pyrite, and elemental Se in soils and waste rock from mining in the Phosphoria Frm. With this data in mind, it is likely that the long term release of Se from the laboratory column experiments is governed by oxidation of Se(−II,0).

4.2. Field experiments

At Wooley Valley, the waste rock dump might be viewed as a chemical reactor where rainwater/snowmelt enters the dump, percolates through and reacts with the waste shale, and exits at the seep. The plot of Se concentration versus time at the seepage outlet of the dump (Fig. 5b) is very similar to the plot of Se concentration at the outlet of the plug flow reactors (Fig. 3). Because of the similarity in output data trends and processes between the laboratory and field experiments, it is tempting to use the same procedure (Fig. 6 and Eqs. (2)–(5)) to analyze both datasets. However there are differences in 'reactor design' between the laboratory and field experiments that keep the data from being comparable. The differences between the 2 systems include the following:

- Solution flow path: in the laboratory plug flow reactor the solution enters the reactor at one point and, ideally, travels as a plug throughout the length of the column, with each plug arriving at the outlet with the same path length and reaction time. This is not the case for the waste rock dump, where fluid can enter the dump anywhere along its surface, and travel to various depths within the dump. Therefore water that exits the dump at the seepage point is a composite of solutions that travelled along different flow paths.
- Solution flow discharge: in the laboratory plug flow reactor, each plug of solution travels through the column with the same velocity, determined by the pump rate. Discharge is constant, and determined by flow rate and the cross-sectional area of the reactor. In the field, the discharge varies throughout the experiment (Fig. 5a) because it is proportional to the hydraulic head which decreases throughout the season, and the permeability which is variable throughout the heterogeneous dump.

The net result of both factors is that in the field experiment, unlike the plug flow laboratory experiment, all fluid elements will NOT have the same residence time within the reactor, meaning the results cannot be directly comparable.

Instead of using the method of Fig. 6 to calculate the 'field' rate constant for Se release, it is possible to calculate an estimated apparent ***k*** directly from the data (Fig. 7). In our conceptual model, Se is leached from the waste rock, *Se(s)*, and transferred to the solution phase, *Se(aq)*:

$$nSe(s) \rightarrow Se(aq) \quad (9)$$

where the coefficient ***n*** indicates that the stoichiometry of this reaction is unknown. While Se might be oxidized and released from a refractory phase such as elemental Se or a Se-bearing sulfide, it might be adsorbed or re-precipitated into another phase, hence not immediately soluble.

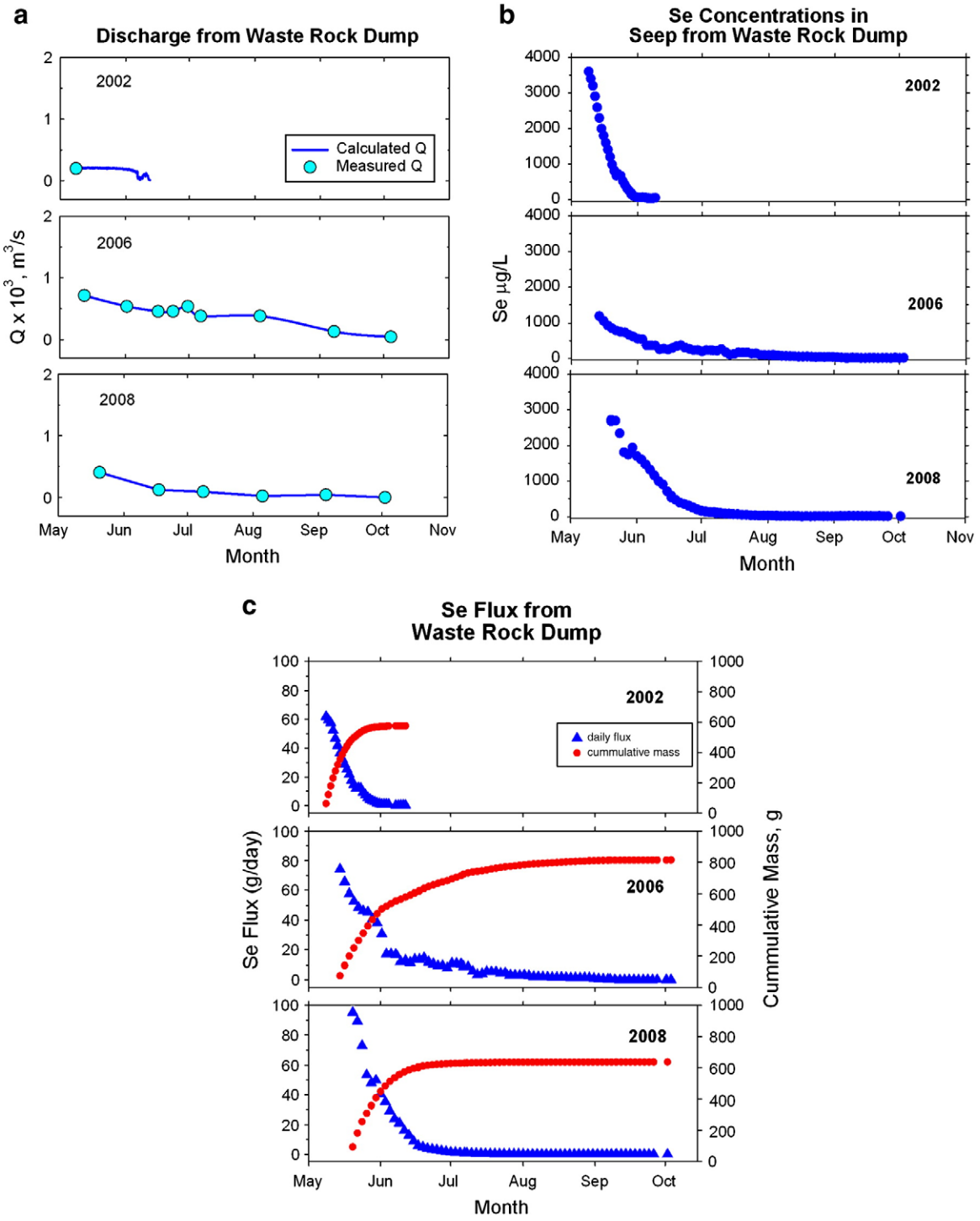

Fig. 5. a. Discharge from the seep at the base of the waste rock dump at Wooley Valley, for 2002, 2006, and 2008. Discharge was measured by measuring stream velocity and the cross-sectional area. The calculated discharge was obtained from a rating curve of discharge vs water level (2002) and the Parshall flume rating equation (2006, 2008). b. Se concentration in the seep from the waste rock dump at Wooley Valley. c. Flux of Se from the waste rock dump at Wooley Valley. Flux is calculated as discharge × concentration.

Laidler, 1987, shows that for any reaction, $2A \rightarrow Z$, the rate of consumption of reactant A, υ_A, is equal to the rate of production of product Z, υ_Z, divided by stoichiometry:

$$\frac{1}{2}\upsilon_A = \upsilon_Z \tag{10}$$

Rate constants follow the same rule:

$$\frac{1}{2}k_A = k_Z \tag{11}$$

Therefore, for the reaction in Eq. (9), the rate constant can be calculated from the production of the product, *Se(aq)*. When the Se concentration in seep discharge (Fig. 5b) is plotted as lnSe(aq) as a function of time (Fig. 7), it fits the linearized, integrated form of a first order rate equation

$$\ln(Se(aq)) = \ln Se(aq)^0 - k_{Se(aq)}t \tag{12}$$

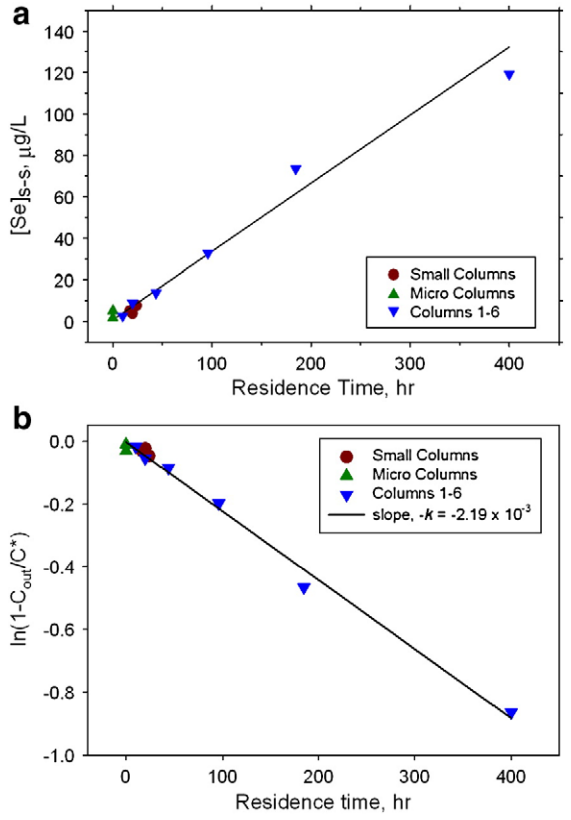

Fig. 6. a. Steady-state Se concentrations $[Se]_{s-s}$, as a function of fluid residence time in the reactor. b. An illustration of the plug flow reactor equation (Eq. (5)), showing the relationship between the extent of reaction at steady-state, C_{out}/C^*, residence time τ, and the rate constant, k.

where the slope of the line is $-k_{Se(aq)}$. Rate constants obtained from this method are 6.35e−3 h^{-1} (2002 data), 1.35e−3 h^{-1} (2006 data), and 2.71e−3 h^{-1} (2008 data).

Although the two calculation methods (Fig. 6 vs Fig. 7) produce rates of the same order of magnitude, it must be noted that the lab and the field rate constants may describe different reactions. In the laboratory experiments, steady-state outlet concentrations were used to calculate the first order rate constant, whereas in the field experiments *all* of the data were used to calculate the rate constant. The field rate constant likely describes a net reaction that includes leaching of both readily soluble and refractory Se, whereas the lab constant describes only leaching of refractory Se. The break in slope in Fig. 7, 2008 data (~2000 h, August 13), may be an artifact because Se concentrations in the samples were at the analytical detection limit of ~15 µg/L.

4.3. Comparison to kinetic rate constants determined from other studies

A number of experiments have been conducted to measure rates of Se oxidation in both laboratory and field settings (Table 3). Most of the studies cited in Table 3 used soils that were collected near the Kesterson Reservoir and its associated agricultural drains. The exceptions were Sarathchandra and Watkinson, 1981, who isolated a bacterium from topsoil alluvium collected from the Whangaehu River on the North Island of New Zealand, and this study.

Many of the studies, especially those of Tokunaga et al., 1994, 1996, and Zawislanski et al., 2003, Zawilslanski and Zavarin, 1996, observed the speciation of Se in their experimental soil materials. They calculate rate constants based upon the appearance of Se(IV + VI) in solution, and/or the extraction of Se(IV + VI) from soil adsorption sites. Thus, rate constants are calculated from concentrations of the oxidized reaction products in solution or soil extracts.

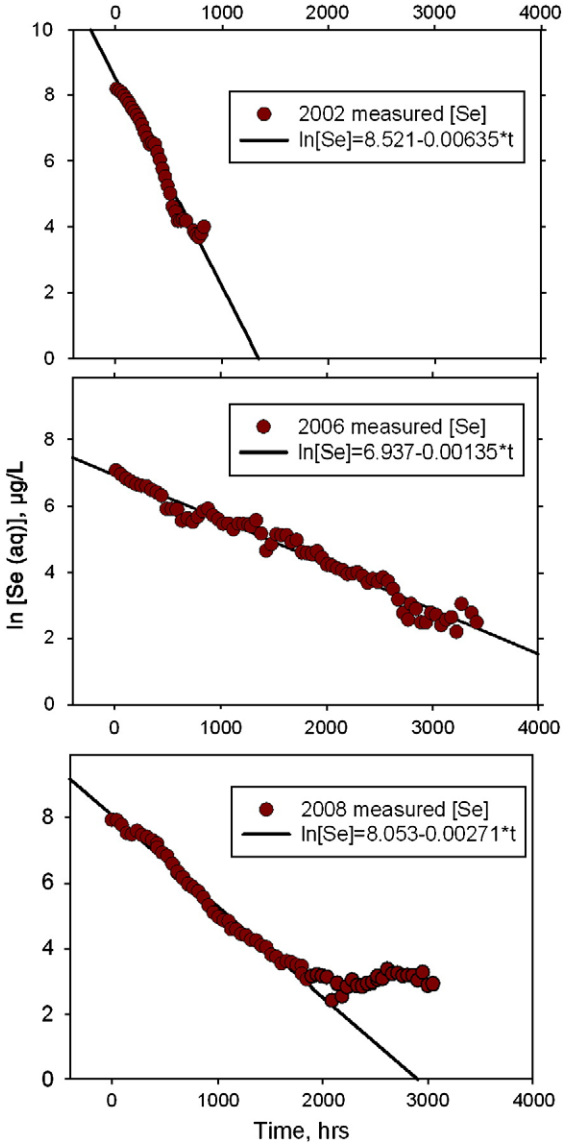

Fig. 7. [Se] vs time, from the outlet seep at the waste rock dump, Wooley Valley, ID.

There are differences in the experimental approach from these studies and the laboratory and field experiments presented here. First, perhaps most importantly, the experiments in this study were flow through experiments, where all of the experiments in Table 3 were either laboratory batch and static soil column incubations, or soil field plot studies. In this study, results were obtained by measuring soluble Se in leachate at the outlet of the soil columns, or at the seepage outlet of the waste dump. Oxygen was not a limiting factor as it might be in ponded water over an underlying soil column, or in a batch experiment. Next, because many of the studies in Table 3 measured Se speciation in their experimental soil materials, they could quote oxidation rates of specific reactants such as $Se_{refractory}$, Se(0), or $Se_{organic}$ starting materials. The rates cited in this present study were for a net reaction, encompassing the oxidation of Se many possible sources (sulfides, Se(0), $Se_{organic}$, and $Se_{adsorbed}$) and did not correct for Se adsorption or reprecipitation.

With this understanding, it is still interesting to compare the rate constants for Se oxidation in Table 3. Rate constants range from a low of 0.004 yr^{-1} (Sarathchandra and Watkinson, 1981) to a high of 108.6 yr^{-1} (Tokunaga et al., 1996). The rate of 0.004 yr^{-1} was observed in a batch reactor for bacterial oxidation of a gray allotrope of Se(0); a red colloidal allotrope of Se(0), was used in the same study and provided

Table 3
Comparison of lab and field rate constants for Se oxidation. Rates are quoted in units provided by the authors, and converted to yr^{-1} for ease of comparison. "n.r." = not reported.

Study	Experimental conditions	Temperature	pH	Eh	Lab rate constant	Field rate constant	Modeled reaction order
This study	Field, waste rock mine dump Phosphoria Frm, SE Idaho	41.1°F[a] (mean annual temp)	7.4–7.8	atm.		0.001–0.006 h^{-1} (*11.8–55.6 yr^{-1}*)	First order
This study	Lab, packed bed reactor columns Flow rate = 1.8–36 cm^3 hr^{-1} Bulk density = 1.2–1.4 g cm^{-3}	Ambient (22–26 deg C)	7.4–7.6	atm.	0.00219 h^{-1} (*19.2 yr^{-1}*)		First order
Zawislanski et al., 2003	Field plot studies of Se oxidation from applied, seleniferous sediments. Rate constant estimated from XANES analysis of Se speciation in sediments. Authors emphasize that rates strongly influenced by early rapid oxidation of organic Se species.	n.r.	7.4–7.7	n.r.		0.82 yr^{-1}	First order
Dowdle and Oremland, 1998	Laboratory experiments with soil slurries spiked with Se(0), and bacterial enrichment cultures	Soil slurries = n.r. enrichment culture = 25 °C	Soil slurries = 7.5	atm.	0.006–0.011/day (*2.2–4.0 yr^{-1}*; soil slurry, bacterial Se(0)) 0.001/day (*0.36 yr^{-1}*; soil slurry, chemical Se(0)) 0.002–0.007/day (*0.73–2.6 yr^{-1}*; bacterial enrichment experiments)		$[Se_{products}]/[Se_{initial}]$/time
Losi and Frankenberger, 1998	Laboratory microcosm experiments, oxidation of soils spiked with Se(0); soils were collected from the San Joaquin Valley, CA, and represented a range of Se levels (0–80 mg/kg). Rates calculated as in Zawilslanski and Zavarin, 1996	n.r.	3 of 4 soils had pH = 7.8–7.9. One soil had pH=2.6.	n.r.	0.04–0.39 yr^{-1}		First order
Tokunaga et al., 1996	Laboratory columns where Se-enriched solutions ponded over Se-free sediments. 25% Se (60 ppm) transferred from solution to sediments in ~50 days(reduction). 60% (36 ppm) of this transferred Se re-oxidized in 2 days after the end of the reduction experiment.	n.r.	n.r.	−400–0 mV, before oxid. began	0.3/day[b] (*108.6 yr^{-1}*)		$[Se_{products}]/[Se_{initial}]$/time
Zawislanski and Zavarin, 1996	Laboratory soil incubations, no enrichment with additional Se.	15–35 °C	6.9–8.0	n.r.	0.058–0.29 yr^{-1} $Se_{organic}$ 0.11–2.4 yr^{-1} $Se_{refractory}$		First order
Tokunaga et al., 1994	Field plots, soil profiles	n.r.	n.r.	n.r.		0.052–0.062 yr^{-1} [b]	$[Se_{products}]/[Se_{initial}]$/time
Masscheleyn et al., 1990	Laboratory incubations, no enrichment with additional Se	28 °C	6.5–9	−200, 0, 200, 400	0.0014 day^{-1}[b] at 0 mV (*0.511 yr^{-1}*)		$[Se_{products}]/[Se_{initial}]$/time
Sarathchandra and Watkinson, 1981	Lab, bacterial enrichment cultures using a gray Se(0) and a red Se(0). The red Se(0) was thought to have a greater surface area, leading to the higher rate constant. Rates calculated as in Dowdle & Oremland, 1998.	28 °C	7	atm.	0.00001/day (*0.004 yr^{-1}*; gray Se)–0.001/day (*0.4 yr^{-1}*; red Se)		$[Se_{products}]/[Se_{initial}]$/time

[a] Mean annual temperature at the Soda Springs airport, ID. Western Regional Climate Center, http://www.wrcc.dri.edu/CLIMATEDATA.html.
[b] Rate constant values not provided in study, but calculated from data as indicated in the right-hand column.

a rate constant of 0.4 yr^{-1}. The authors suggested the low rate was because of the low surface area of the gray Se(0), compared to the red. Dowdle and Oremland, 1998, also experimented with both a red and a gray allotrope of Se(0) but in their work the allotropes were formed by bacterial and chemical reduction, respectively, of Se(IV). Here, the gray form of Se(0) had a rate constant for oxidation ~1 order of magnitude lower than the constant for the red Se(0) (Table 3). The highest rate constant for Se oxidation, 108.6 yr^{-1}, was measured in laboratory experiments where 3 mM solutions of Se(VI) were ponded over uncontaminated soils for ~50 days. During this time reduction of Se (VI) to Se(0) was observed. The rate constant for Se oxidation was calculated for the short-term reoxidation that occurred within the 2 days following the end of the reduction experiment, when the wet sediments were collected and stored in air (Tokunaga et al., 1996). In these experiments the high concentration of Se in the experiment, together with the short (50 day) reduction time, may have led to a high concentration of easily re-oxidized Se and hence a high rate constant.

The rate constants derived from this study, from both field and laboratory experiments, are ~1 order of magnitude higher than the highest constants reported from Dowdle and Oremland, 1998, and Zawilslanski and Zavarin, 1996, but lower than the highest constant reported, 108.6 yr^{-1}. Dowdle and Oremland, 1998, reported a constant of 2.2–4.0 yr^{-1} for oxidation of a red, bacterially precipitated form of Se(0); Zawislanski and Zavarin reported a constant of 2.4 yr^{-1} for oxidation of a refractory Se phase in laboratory incubations of Se contaminated soils. Both of these experiments were batch

experiments where the authors made the effort to keep the sample aerated, but they were not flow through experiments. While the 'refractory Se' phase was not identified, it is likely to contain Se(0) and Se-sulfide phases.

The comparison between rate constants of this study (11.8–55.6 yr^{-1}) and those of Table 3 for Se(0) oxidation (2.4–108.6 yr^{-1}) suggest that it may be Se(0) that is oxidizing to a soluble Se. This is consistent with the previously noted observations of Grauch et al., 2004, and Ryser et al., 2006, who reported that the most common host of Se in the Meade Peak shale is elemental Se, Se(0).

5. Conclusions

Se leaching from shales of the Meade Peak member of the Phosphoria Formation was observed in both field and laboratory experiments. In both sets of experiments, Se concentration in outlet solutions was high, initially, and decreased over time to a steady-state concentration. Two methods were used to estimate the rate constant: In the laboratory experiments, a linear plot of outlet Se concentration versus residence time was used to estimate a first order rate constant of 2.19e−3 h^{-1}. In the field, a plot of ln[Se] versus time was fit with first order rate model, where $\boldsymbol{k}$ = 6.35e−3 h^{-1} (2002), 1.35e−3 h^{-1} (2006), and 2.71e−3 h^{-1} (2008).

The rate constants estimated by this study are within an order of magnitude of other rate constants, cited in the literature, for oxidation of bacterially precipitated Se(0). While the methods described in this study produce a constant for a net, overall rate, it has been shown that the predominate Se-bearing phase in the Meade Peak shale is elemental Se, Se(0). Therefore, the similarity between the new rate constants presented here to known rate constants for Se(0) oxidation suggests that oxidation of Se(0) in the Meade Peak shale controls the concentration of Se in waters draining dumps of waste rock that have resulted from mining activities in the Phosphoria Fm. in southeastern Idaho.

Acknowledgements

Funding for this work was provided by the U.S. Geological Survey Minerals Research Program (LLS) and the U.S. Forest Service ECAP/AML program (MCA). Both authors wish to thank Kay Laird (USFS-RMRS, Logan UT) for analyzing samples for Se by HGAAS; as well as Chuck Coronella, Dept. Chemical Engineering, University of Nevada, Reno, for assistance with analysis of data from a plug flow reactor. Ralph Seiler and Dave Naftz, of the U.S.Geological Survey, and 2 anonymous reviewers provided very helpful reviews. Any use of trade, product, or firm names is for descriptive purposes only and does not imply endorsement by the U.S. Government.

References

Agrium Conda Phosphate Operations, Astaris LLC, Bureau of Land Management, Idaho Department of Lands, J.R. Simplot Company, Monsanto Company, and United States Forest Service, 2005. Selenium Management Practices, A Cooperative Document, http://giscenter-ims.isu.edu/SISP/reports/Se%20Management%20Practices%202006-2005.pdf, accessed June, 2009.

Amacher, M.C., Herring, J.R., Stillings, L.L., 2001. Total recoverable selenium and other elements by HNO_3 and $HClO_4$ digestion and other soil characterization data from Wooley Valley Units 3 and 4 waste rock dumps and Dairy Syncline lease area soils, southeast Idaho. Open-File Report 01-69. U.S. Geological Survey. 65 pp.

Briggs, Paul H., 2002. The determination of forty elements in geological and botanical samples by inductively coupled plasma-atomic emission spectrometry. Analytical Methods for Chemical Analysis of Geologic and Other Materials. In: Taggat Jr., Joseph E. (Ed.), Open-File Report 02-223, Chapter G. U.S. Geological Survey.

Buck, Brian W., Jones, Jeffery L., 2002. Interagency/industry coordination to respond to Selenium contamination at phosphate mines in southeastern Idaho. http://www.fs.fed.us/geology/buck-jones.pdf, accessed January, 2009.

Carter, R.W., Davidian, J., 1968. General procedure for gaging streams. Techniques of Water-Resources Investigations. U.S. Geological Survey. book 3, chap A6, 13 pp.

Dowdle, P.R., Oremland, R.S., 1998. Microbial oxidation of elemental Selenium in soil slurries and bacterial cultures. Environ. Sci. Technol. 32, 3749–3755.

Engberg, R.A., Sylvester, M.A., 1993. Concentrations, distribution, and sources of Selenium from irrigated lands in western United States. J. Irrig. Drain. Eng. 119, 522–536.

Flint, Alan L., Flint, Lorraine E., 2002. Chapter 2.2: Particle Density. In: Dane, Jacob H., Topp, G. Clarke (Eds.), SSSA Book Series, vol. 5. Soil Science Society of America, Inc., pp. 229–240.

Grauch II, R., Desborough, G.A., Meeker, G.P., Foster, A.L., Tysdal, R.G., Herring, F.R., Lowers, H.A., Ball, B.A., Zielinski, R.A., Hohnson, E.A., 2004. Petrogenesis and mineralogic residence of selected elements in the Meade Peak Phosphatic Shale member of the Permian Phosphoria formation, southeast Idaho. In: Hein, James R. (Ed.), Life Cycle of the Phosphoria Formation. Handbook of Exploration and Environmental Geochemistry, vol. 8. Elsevier, pp. 189–226.

Greater Yellowstone Coalition, 2006. Animal Deaths, Local Extinctions, and Human Health Concerns in the Phosphate Mining Area of Southeast Idaho. Fact sheet available at http://www.greateryellowstone.org/media/pdf/SmokyMine-Animal_Extinct.pdf, accessed January, 2009.

Hachiya, K., Sasaki, M., Ikeda, T., Mikami, N., Yasunaga, 1984. Static and kinetic studies of adsorption–desorption of metal ions on a y-Al, O, surface 2. Kinetic study by means of pressure-jump technique T. J. Phys. Chem. 88, 27–31.

Hein, James R., McIntyre, Brandie, Perkins, Robert B., Piper, David Z., Evans, James, 2002. Composition of the Rex Chert and associated rocks of the Permian Phosphoria Formation: Soda Springs Area, SE Idaho. Open-File Report 02-345. U.S. Geological Survey. 30 pp.

Hein, J.R., Perkins, R.B., McIntyre, B.R., 2004. Evolution of thought concerning the origin of the Phosphoria Formation, western US Phosphate Field. In: Hein, James R. (Ed.), Life Cycle of the Phosphoria Formation: From Deposition to Post-Mining Environment: Handbook of Exploration and Environmental Geochemistry, vol. 8, pp. 19–42.

Herring, J.R., Grauch, R.I., Siems, D.F., Tysdal, R.G., Johnson, E.A., Zielinski, R.A., Desborough, G.A., Knudsen, A., Gunter, M.E., 2001. Chemical composition of strata of the Meade Peak phosphatic shale member of the Permian Phosphoria Formation. Open-File Report 01-195. U.S. Geological Survey. 72 pp.

Hill Jr., Charles G., 1977. An Introduction to Chemical Engineering Kinetics and Reactor Design. John Wiley and Sons, NY. 594 pp.

Laidler, Keith J., 1987. Chemical Kinetics, 3rd ed., Harper & Row, Publishers, Inc. 531 pp.

Lamothe, Paul J., Meier, Allen L., Wilson, Stephen A., 2002. The determination of forty-four elements in aqueous samples by inductively coupled plasma-mass spectrometry. Analytical Methods for Chemical Analysis of Geologic and Other Materials. In: Taggat Jr., Joseph E. (Ed.), Open-File Report 02-223. U.S. Geological Survey. Chapter H.

Lemly, A.D., 2002. Selenium Assessment in Aquatic Ecosystems. Springer. 160 pp.

Losi, M.E., Frankenberger Jr., W.T., 1998. Microbial oxidation and solubilization of precipitated elemental Selenium in soil. J. Environ. Qual. 27, 836–843.

Mackowiak, C.L., Amacher, M.C., 2008. Soil sulfur amendments suppress selenium uptake by alfalfa and western wheatgrass. J. Environ. Qual. 37, 772–779.

Martens, D.A., Suarez, D.L., 1997. Selenium speciation of marine shales, alluvial soils, and evaporation basin soils of California. J. Environ. Qual. 26, 424–432.

Masscheleyn, P.H., Delaune, R.D., Patrick, W.H., 1990. Transformations of Selenium as affected by sediment oxidation–reduction potential and pH. Environ. Sci. Technol. 24, 91–96.

McNeal, James M., Balistrieri, Laurie S., 1989. Geochemistry and occurrence of selenium; an overview. In: Jacobs, L.W. (Ed.), Selenium in Agriculture and the Environment, vol. 23. SSSA Special Publication, pp. 1–13.

Perkins, R.B., Foster, A.L., 2004. Mineral affinities and distribution of selenium and other trace elements in black shale and phosphorite of the Phosphoria Formation. Life Cycle of the Phosphoria Formation: From Deposition to Post-Mining Environment. In: Hein, James R. (Ed.), Handbook of Exploration and Environmental Geochemistry, vol. 8. Elsevier B.V., pp. 251–295.

Piper, D.Z., 2001. Marine chemistry of the Permian Phosphoria Formation and Basin, southeast Idaho. Econ. Geol. 96, 599–620.

Piper, D.Z., 1999. Trace elements and major-element oxides in the Phosphoria Formation at Enoch Valley, Idaho—Permian sources and current reactivities. Open File Report 99-163. U.S. Geological Survey. 66 pp.

Presser, T., 1994. The Kesterson effect. Environ. Manage. 18, 437–454.

Ryser, Amy L., Strawn, Daniel G., Marcus, Matthew A., Johnson-Maynard, Jodi L., Gunter, Mickey E., Möller, Gregory, 2005. Micro-spectroscopic investigate of selenium-bearing minerals from the Western US Phosphate Resource Area. Geochem. Trans. 6, 1–11.

Ryser, Amy L., Strawn, Daniel G., Marcus, Matthew A., Johnson-Maynard, Jodi L., Möller, Gregory, 2006. Microscopically focused synchrotron X-ray investigation fo selenium speciation in soils developing on reclaimed mine lands. Environ. Sci. Technol. 40, 462–467.

Sarathchandra, S.U., Watkinson, J.H., 1981. Oxidation of elemental Selenium to selenite by *Bacillus megaterium*. Science 211, 600–601.

Seiler, Ralph L., Skorupa, Joseph P., Naftz, David L., Nolan, Thomas B., 2003. Irrigation-induced contamination of water, sediment, and biota in the western United States—synthesis of data from the National Irrigation Water Quality Program. Professional Paper, vol. 1655. U.S. Geological Survey. 123 pp.

Stillings, L., Amacher, M., 2004. Selenium attenuation in a wetland formed from mine drainage in the Phosphoria Formation, southeast Idaho. Life Cycle of the Phosphoria Formation: From Deposition to the Post-Mining Environment. In: Hein, James R. (Ed.), Handbook of Exploration and Environmental Geochemistry, vol. 8. Elsevier B.V., Amsterdam, pp. 467–482.

Stillings, Lisa L., Amacher, Michael C., submitted for publication. Chemistry and discharge of seeps and surface waters draining mined waste rock from the Meade Peak Phosphatic Shale, Phosphoria Formation, Wooley Valley Unit 4, southeastern Idaho, USA. U.S. Geological Survey Open-File Report.

Tetra Tech EM, Inc., 2002. Final Area Wide Human Health and Ecological Risk Assessment, Selenium Project Southeast Idaho Phosphate Mining Resource Area. Contract Number C023, Task Order AWI-00-01. available at http://giscenter-ims.isu.edu/SISP/Area_Wide_Reports.html, accessed June, 2009.

Tokunaga, Tetsu K., Pickering, Ingrid J., Brown Jr., Gordon E., 1996. Selenium transformations in ponded sediments. Soil Sci. Soc. Am. J. 60, 781–790.

Tokunaga, T.K., Zawislanksi, P.T., Johannis, P.W., Benson, S., 1994. Field investigations of selenium speciation, transformation, and transport in soils from Kesterson Reservoir and Lahontan Valley. In: Benson, S. (Ed.), Selenium in the Environment. Marcel Dekker, Inc., pp. 119–138.

van Leeuwen, Herman P., 2008. Eigen kinetics in surface complexation of aqueous metal ions. Langmuir 24, 11718–11721.

Zawilslanski, P.T., Zavarin, M., 1996. Nature and rates of selenium transformations: a laboratory study of Kesterson Reservoir soils. Soil Sci. Soc. Am. J. 60, 791–800.

Zawislanski, Peter T., Benson, Sally M., Terbert, Robert, Borglin, Sharon E., 2003. Selenium speciation, solubility, and mobility in land-disposed dredged sediments. Environ. Sci. Technol. 37, 2415–2420.

Zhang, P.C., Sparks, D.L., 1989. Kinetics and mechanisms of molybdate absorption/desorption at the goethite/water interface using pressure-jump relaxation. Soil Sci. Soc. Am. J. 53, 1028–1034.